Asian Journal of Chemistry; Vol. 29, No. 5 (2017), 975-982

ASIAN JOURNAL OF CHEMISTRY

https://doi.org/10.14233/ajchem.2017.20351

Synthesis and Spectroscopic Characterization of Ruthenium Polypyridyl Complexes Containing 1,6-*bis*(Benzylidene)hexanediamine as Ligand

ARCHANA CHOUBEY[1,*], SATYENDRA N. SHUKLA[2], PRATIKSHA GAUR[2] and CHETNA ACHARYA[1]

[1]Department of Chemistry, Sagar Institute of Science Technology & Research, Sikandrabad, Ratibad, Bhopal-462 044, India
[2]Coordination Chemistry Research Lab, Department of Chemistry, Government Model Science College, Jabalpur-482 001, India

*Corresponding author: E-mail: choubey.a64@gmail.com

Received: 15 October 2016; *Accepted*: 13 January 2017; *Published online*: 10 March 2017; AJC-18284

A novel bidentate ligand 1,6-*bis*(benzylidene)hexanediamine was synthesized and its eight ruthenium *bis*(bypyridine)sulphoxide complexes with the general formula [*cis*/*trans*-$RuCl_2(SO)_2$(N-N)](L); were SO = dimethyl sulphoxide (DMSO)/tetramethylene sulphoxide (TMSO), (N-N) = 1,10-phenanthroline/2,2'-bipyridyl, (L) = bridging ligand were synthesized. These complexes were characterized by elemental analysis, IR, UV/visible, ^{1}H NMR, ^{13}C NMR and 2D NMR spectroscopy. All complexes were found to show antibacterial property against *E. coli* and the pyridal ligands co-ordinate through a Ru–N bond in all cases.

Keywords: Ruthenium bypyridine, Hexanediamine, Sulphoxide, Phenanthroline.

INTRODUCTION

During the last decades, ruthenium(II)-based polypyridyl complexes have been the object of an active field of research [1]. Ruthenium(II)-polypyridyl complexes belong to one of the most thoroughly investigated classes of coordination compounds, since they offer a variety of technologically relevant properties, namely, photophysical, redox and charge transfer characteristics [2]. These properties have prompted the use of ruthenium(II) complexes as photosensitizers across diverse light-driven applications such as artificial photosynthesis [3], photocatalytic production of hydrogen [4], dye-sensitized solar cells [5], photon-induced switches [6] and molecular machines and devices [7].

Recently, a large interest has grown in ruthenium polypyridyl complexes as a possible alternative to the use of classical platinum chemotherapy. Some examples of these compounds are $Ru(tpy)Cl_3$ and α-$[Ru(azpy)_2Cl_2]$ (azpy = 2-phenylazopyridine). $Ru(tpy)Cl_3$ shows a pronounced *in vitro* cytotoxicity and exhibits antitumor activity. The compound α-$[Ru(azpy)_2Cl_2]$ has been reported to show a remarkably high cytotoxicity, even more pronounced than cisplatin in most of the tested cell lines. The increased amount of possible binding modes of ruthenium polypyridyl complexes to DNA as compared to those of the first generations of platinum drugs, including intercalation of the ligands between two parallel base pairs, could be crucial in order to overcome resistance to cisplatin. In addition, a number of ruthenium complexes, such as NAMI-A, $[H_2im][trans\text{-}RuCl_4(DMSO\text{-}S)(Him)]$ (Him = imidazole; DMSO = dimethyl sulfoxide), have shown to display an antimetastatic activity, which has not been observed in the case of the routinely used platinum compounds [8].

1,6-Hexanediamine is a well known antimicrobial agent and used in dye-sensitized cell [9,10]. Here it will be of interest to synthesize some new molecule which has an excellent tendency to inhibit the growth of pathogenic bacteria. Thus to achieve this goal, we have coupled 1,6-hexanediamine with benzaldehyde to give rise to a novel bidentate spacer. We have explored the reaction of this novel spacer with different ruthenium sulphoxide bipyridyl compounds, resulting in the formation of dinuclear complexes with enhanced antibacterial activity.

EXPERIMENTAL

{^{13}C-^{1}H}^{2}D NMR, ^{1}H NMR and ^{13}C NMR spectra were recorded on D6-DRX-300 MHz Bruker, spectrophotometer with TMS as the internal standard. Chemical shifts are expressed inparts per million FAB-Mass spectra of ligand and complexes were recorded on JMS SX-102-Jeol Mass spectrometer using NBA as matrix. FTIR spectrum in the range 4000-400 cm^{-1} were recorded in KBr pellets on Shimadzu-8400 PC. The absorption spectra were recorded on Systronics 2201 UV-visible double beam spectrophotometer equipped with P.C. All chemicals were of A.R. grade and purified by standard procedures.

Synthesis of 1,6-*bis*(benzylidene)hexanediamine ligand (BDH): As shown in Fig. 1, the ligand BDH was synthesized using hexanediamine (1 g; 1 mmol) in 20 mL ethanol. To this solution benzaldehyde (1.749 mL; 2 mmol) was added and the reaction mixture was kept on stirring for 4 h in an inert atmosphere. Cream colour solid was recovered which was filtered and dried under reduced pressure. The solid was recrystallized in ethanol:methanol:acetone, 1:1:1 (v/v) mixture.

Cream solid, Yield 85.31 % m.p.: 115 °C; ^{1}H NMR (300 MHz; D_2O, δ): 8.1 (4H, s, H_1), 7.7 (4H, s, H_2), 7.3, (2H, s, H_3), 8.8 (H_4, –CH=N), 3.6 (4H, s, H_5, -CH_2), 3.2 (4H, s, H_6), 2.1 (4H, s, H_7); ^{13}C NMR (300 MHz, δ D_2O) C_1-130.5, C_2-129.0, C_3-130.0, C_8-129.0, (Ar-C), C_4-161.0 (–CH=N), C_5-61, C_6-51, C_7-30 (CH_2). Anal. calcd. (%) for $C_{20}H_{18}N_2$: C, 83.10; H, 6.25; N, 9.62, Found (%): C, 83.88; H, 6.33; N, 9.78.

Synthesis of complexes

Synthesis of complex is performed in three steps: The four starting complexes were prepared by the method reported by Evans *et al.* [11] and Alessio *et al*. [12-14]. These complexes are [*cis*,*fac*-$RuCl_2(DMSO\text{-}S)_3(DMSO\text{-}O)$, *trans*-$RuCl_2(DMSO)_4$, *cis*-$RuCl_2(TMSO)_4$, *trans*-$RuCl_2(TMSO)_4$. Recrystallized starting complex was dissolved in small volume (about 5 mL) of DMSO/TMSO. In this solution 1,10-phenanthroline/2,2'-bipyridyl dissolved in about 10 mL acetone was added in 1:1 molar ratio. The above reaction mixture was refluxed for 1-2 h and the colour of the solution changed to red orange. This solution on vacuum evaporation yielded red orange solid which was recrystallized with 1:1 (v/v) mixture of diethyl ether: acetone. Total eight precursors [*cis*-$RuCl_2(DMSO)_2(phen)$]; [*trans*-$RuCl_2(DMSO)_2(phen)$]; [*cis*-$RuCl_2(DMSO)_2(bpy)$]; [*trans*-$RuCl_2(DMSO)_2(bpy)$]; [*cis*-$RuCl_2(TMSO)_2(phen)$]; [*trans*-$RuCl_2(TMSO)_2(phen)$]; [*cis*-$RuCl_2(TMSO)_2(bpy)$]; [*trans*-$RuCl_2(TMSO)_2$bpy] were synthesized.

Synthesis of dinuclear complexes: The recrystallized precursor (1 mmol) was dissolved in minimum quantity of DMSO/TMSO. The spacer 1,6-*bis*(benzylidene)hexanediamine, (1 mmol) dissolved in 10 mL of acetone was mixed to the above reaction mixture and kept under refluxed for 1-8 h in an inert atmosphere. Colour of the reaction mixture changed. The above solution was decanted and evaporated under vacuum resulting into microcrystals, which were washed several times with acetone and recrystallized from diethyl ether:acetone, 1:1(v/v) mixture. In total, eight complexes were synthesized.

[{*cis*-$RuCl_2$(DMSO)phen}$_2$(μ-BDH)]·DMSO: Dark red solid, Yield, 87.10 %; m.p.: 160 °C; UV-visible (H_2O) (λ_{max}, nm, ε, mol^{-1} cm^{-1}): 604 (145), 523 (292), 490 (338), 454 (467), 430 (674), 410 (746), 392 (829), 385 (846). ^{1}H NMR (300 MHz. D_2O, δ): 9.91 (HC=N), 3.41 (12H, CH_3), 2.42 (6H, CH_3), 3.6, 2.5, 2.0 (12H, t, CH_2); ^{13}C NMR (300 MHz, D_2O, δ): 151.5 (–CH=N) 46.0, 36.5 (-S-C), 28.0, 34.3, 47.5 (–CH_2); IR (KBr, cm^{-1}): 2895 (stretching for ν(CH_2)$_6$), 1620 (stretching for ν –CH=N); MS (*m/z*): $[RuCl]^+$ = 136, $[C_2H_6ClOSRu]^+$ = 214, $[C_{12}H_8N_2ClRu]^+$ = 316, $[C_{14}H_{14}N_2OSClRu]^+$ = 394, $[C_{34}H_{38}N_4OSClRu]^+$ = 687, $[C_{48}H_{52}N_6O_2S_2Cl_3Ru_2{}^{101}]^+$ = 1231, $[C_{48}H_{52}N_6O_2S_2Cl_3Ru_2{}^{102}]^+$ = 1233; Anal. calcd. (%) for $C_{50}H_{58}N_6O_3S_3Ru_2Cl_4$: C, 48.05; H, 4.10; N, 6.10; S, 7.42; Ru, 16.01, Found (%): C, 48.78; H, 4.75; N, 6.83; S, 7.81; Ru, 16.42.

[{*trans*-$RuCl_2$(DMSO)phen}$_2$(μ-BDH)]·DMSO: Red brown solid, Yield, 95.38 %; m.p.: 165 °C; UV-visible (H_2O) (λ_{max}, nm, ε, mol^{-1}cm^{-1}): 625 (101), 540 (265), 490 (338), 467 (425), 449 (565), 432 (652), 425 (689); ^{1}H NMR (300 MHz, D_2O, δ): 9.80 (–CH=N), 2.90 (12H, CH_3), 2.31 (6H, CH_3), 1.4, 1.6, 2.4 (12H, t, CH_2); ^{13}C NMR (300 MHz, D_2O, δ): 152.0 (–CH=N), 44.0, 36.0 (S-C), 25.0, 26.0, 43.0. (CH_2); IR (KBr, cm^{-1}) 2900 (s, ν(CH_2)$_6$), 1619 (s, ν –CH=N); MS (*m/z*): $[RuCl]^+$ = 136, $[C_2H_6ClOSRu]^+$ = 214, $[C_{12}H_8N_2ClRu]^+$ = 316, $[C_{14}H_{14}N_2OSClRu]^+$ = 394, $[C_{34}H_{38}N_4OSClRu]^+$ = 687, $[C_{48}H_{52}N_6O_2S_2Cl_3Ru_2{}^{101}]^+$ = 1231, $[C_{48}H_{52}N_6O_2S_2Cl_3Ru_2{}^{102}]^+$ = 1233; Anal. calcd. (%) for $C_{50}H_{58}N_6O_3S_3Ru_2Cl_4$: C, 48.05; H, 4.10; N, 6.10; S, 7.42; Ru, 16.01, Found (%): C, 48.79; H, 4.76; N, 6.81; S. 7.82; Ru, 16.41.

[{*cis*-$RuCl_2$(DMSO)bpy}$_2$(μ-BDH)]·DMSO: Brown solid, Yield, 93.00 %; m.p.: 169 °C; UV-visible (H_2O) (λ_{max}, nm, ε, mol^{-1}cm^{-1}): 604 (145) 565 (208) 503 (290), 496 (348), 468 (496), 430 (674) 415 (698) ^{1}H NMR (300 MHz, D_2O, δ): 9.91 (-CH=N), 3.30 (12H, CH_3) 2.41 (6H, CH_3) 1.5, 2.3 2.9 (t, 12H, CH_2); ^{13}C NMR (300 MHz, δ D_2O): 152.3 (–CH=N), 47.1, 37.5 (S-C), 26.2, 28.0, 47.0 (CH_2); IR (KBr, cm^{-1}): 2898 (s, ν(CH_2)$_6$), 1600 (s, ν –CH=N); MS (*m/z*): $[RuCl]^+$ = 136, $[C_2H_6ClOSRu]^+$ = 214, $[C_{10}H_8N_2ClRu]^+$ = 292, $[C_{12}H_{14}N_2OSClRu]^+$ = 370, $[C_{32}H_{38}N_4OSClRu]^+$ = 663, $[C_{44}H_{52}N_6O_2S_2Cl_3Ru_2{}^{101}]^+$ = 1069, $[C_{44}H_{52}N_6O_2S_2Cl_3Ru_2{}^{102}]^+$ = 1071; Anal. calcd. (%) for $C_{46}H_{58}N_6O_3S_3Ru_2Cl_4$: C, 46.01; H, 4.10; N, 7.24; S, 8.15; Ru, 17.05; Found (%): C, 46.70; H, 4.94; N, 7.10; S, 8.13; Ru, 17.09.

[{*trans*-$RuCl_2$(DMSO)bpy}$_2$(μ-BDH)]·DMSO: Dark brown solid, Yield, 87.87 %; m.p.: 170 °C; UV-visible (H_2O) (λ_{max}, nm, ε, mol^{-1} cm^{-1}): 614 (135), 579 (178), 526 (295), 480 (345), 469 (423), 458 (468), 430 (674), 410 (746); ^{1}H NMR (300 MHz, D_2O, δ): 9.89 (–CH=N), 2.90 (12H, CH_3), 2.38 (6H, CH_3) 1.4, 2.1, 3.0 (t, 12H, CH_2); ^{13}C NMR (300 MHz, D_2O, δ): 153.0 (–CH=N), 44.5, 38.2 (S-C), 24.5, 29.2, 43.0 (CH_2); IR (KBr, cm^{-1}): 2900(s, (CH_2)$_6$) 1610 (s, –CH=N); MS (*m/z*): $[RuCl]^+$ = 136, $[C_2H_6ClOSRu]^+$ = 214, $[C_{10}H_8N_2ClRu]^+$ = 292, $[C_{12}H_{14}N_2OSClRu]^+$ = 370, $[C_{32}H_{38}N_4OSClRu]^+$ = 663, $[C_{44}H_{52}N_6O_2S_2Cl_3Ru_2{}^{101}]^+$ = 1069, $[C_{44}H_{52}N_6O_2S_2Cl_3Ru_2{}^{102}]^+$ = 1071; Anal. calcd. (%) for $C_{46}H_{58}N_6O_3S_3Ru_2Cl_4$: C, 46.01; H, 4.10; N, 7.24; S, 8.15; Ru, 17.05; Found (%): C, 46.72; H, 4.91; N, 7.11; S, 8.11; Ru, 17.05.

[{*cis*-$RuCl_2$(TMSO)phen}$_2$(μ-BDH)]·TMSO: Dark orange solid, Yield, 93.75 %; m.p.: 172 °C; UV-visible (H_2O)

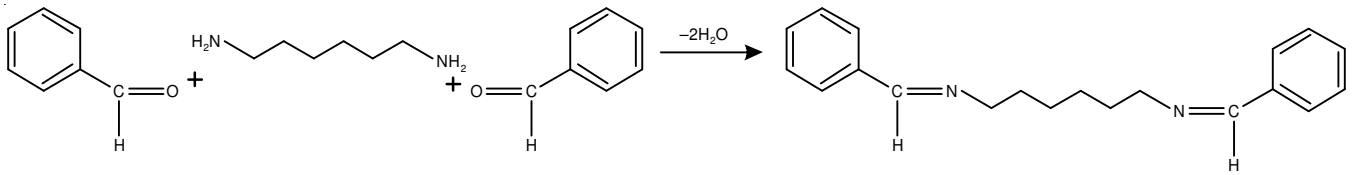

Fig. 1. Reaction scheme for ligand preparation

(λ_{max}, nm, ε, $mol^{-1}cm^{-1}$): 621 (105), 549 (260), 497 (392), 476 (467), 458 (468), 448 (560), 412 (729), 385 (842); ^{1}H NMR (300 MHz; D_2O δ): 9.91 (–CH=N), 4.20 (8H, S-CH_2), 3.60 (4H, S-CH_2), 3.32 (12H, S-C-CH_2), 2.1, 2.9, 3.8 (t, 12H, CH_2); ^{13}C NMR (300 MHz, D_2O, δ) 151.8 (–CH=N)) 47.8, 40.5 (S-C), 25.2 (S-C-C) 30.2, 41.3, 48.0 (CH_2); IR (KBr, cm^{-1}): 2904 (s $(CH_2)_6$) 1612 (s, –CH=N); MS (*m/z*): $[RuCl]^+$ = 136, $[C_4H_8ClOSRu]^+$ = 240, $[C_{12}H_8N_2ClRu]^+$ = 316, $[C_{16}H_{16}N_2OSClRu]^+$ = 420, $[C_{36}H_{40}N_4OSClRu]^+$ = 713, $[C_{52}H_{56}N_6O_2S_2Cl_3Ru_2^{101}]^+$ = 1169, $[C_{52}H_{56}N_6O_2S_2Cl_3Ru_2^{102}]^+$ = 1171;. Anal. calcd. (%) for $C_{56}H_{64}N_6O_3S_3Ru_2Cl_4$: C, 51.10; H, 4.75; N, 6.10; S, 7.25; Ru, 15.35; Found (%): C, 51.37; H, 4.93; N, 6.42; S, 7.35, Ru, 15.44.

[{*trans*-$RuCl_2$(TMSO)phen}$_2$(μ-BDH)]·TMSO: Dark brown solid, Yield, 91.93 %; m.p.: 161 °C; UV-visible (H_2O) (λ_{max}, nm, ε, $mol^{-1}cm^{-1}$): 610 (150), 575 (198), 510 (295), 492 (378), 479 (450), 464 (508), 448 (560), 425 (689), 390 (830); ^{1}H NMR (300 MHz; D_2O, δ): 9.82 (–CH=N), 3.90 (8H, S-CH_2), 3.53 (4H, S-CH_2), 3.45 (12H, S-C-CH_2), 1.9, 2.5, 3.4 (t, 12H, CH_2); ^{13}C NMR (300 MHz, D_2O, δ): 152.2 (–CH=N), 43.0, 40.4 (S-C), 24.8 (S-C-C), 29.8, 40.3, 47.9 (CH_2); IR (KBr, cm^{-1}): 2892 (s, $(CH_2)_6$), 1610 (s, –CH=N); MS (*m/z*):$[RuCl]^+$ = 136, $[C_4H_8ClOSRu]^+$ = 240, $[C_{12}H_8N_2ClRu]^+$ = 316, $[C_{16}H_{16}N_2OSClRu]^+$ = 420, $[C_{36}H_{40}N_4OSClRu]^+$ = 713, $[C_{52}H_{56}N_6O_2S_2Cl_3Ru_2^{101}]^+$ = 1169, $[C_{52}H_{56}N_6O_2S_2Cl_3Ru_2^{102}]^+$ = 1171; Anal. calcd. (%) for $C_{56}H_{64}N_6O_3S_3Ru_2Cl_4$: C, 51.10; H, 4.75; N, 6.10; S, 7.25; Ru, 15.35; Found (%): C 51.37; H 4.91; N 6.41; S 7.36; Ru 15.45.

[{*cis*-$RuCl_2$(TMSO)$_2$bpy}$_2$(μ-BDH)]·TMSO: Red brown solid, Yield: 93.97 %; m.p.: 167°; UV-visible (H_2O) (λ_{max}/nm, ε in $mol^{-1}cm^{-1}$): 625 (101) 568 (198), 505 (294) 490 (338) 468 (420), 446 (578) 428 (675) 408 (743), 390 (830); ^{1}H NMR (300 MHz, δ D_2O): δ (–CH=N) 9.82 δ (S-CH_2) 4.18 (8H)3.61 (4H) δ (S-C-CH_2) 3.44 (12H) δ (CH_2) 1.8, 2.4, 3.1 (t, 12H); ^{13}C NMR (300 MHz, δ D_2O) δ (–CH=N) 151.7 δ (S-C) 48.0, 40.5 δ (S-C-C) 25.4 δ (CH_2) 31.4, 41.2, 48.8; IR (KBr, cm^{-1}) ν$(CH_2)_6$ 2895(s) ν(–CH=N) 1614(s); MS (*m/z*): $[RuCl]^+$ = 136, $[C_4H_8ClOSRu]^+$ = 240, $[C_{10}H_8N_2ClRu]^+$ = 292, $[C_{14}H_{16}N_2OSClRu]^+$ = 396, $[C_{34}H_{40}N_4OSClRu]^+$ = 689, $[C_{48}H_{56}N_6O_2S_2Cl_3Ru_2^{101}]^+$ = 1121, $[C_{48}H_{56}N_6O_2S_2Cl_3Ru_2^{102}]^+$ = 1123; Anal. calcd. (%) for $C_{52}H_{64}N_6O_3S_3Ru_2Cl_4$: C, 49.05; H, 5.24; N, 6.25; S, 7.44; Ru, 16.30; Found (%): C 49.52 H 5.11 N 6.66 S 7.63 Ru 16.03.

[{*trans*-$RuCl_2$(TMSO)bpy}$_2$(μ-BDH)]·TMSO: Red orange solid, Yield %:0.050 g (93.46 %) M.p.:171; UV-visible (H_2O) (λ_{max}/nm, ε in $mol^{-1}cm^{-1}$): 648 (110) 549 (260), 497 (392) 478 (455), 448 (560) 429 (672) 402 (735), 398 (789); ^{1}H NMR (300 MHz, δ D_2O): δ (–CH=N) 9.83 δ (S-CH_2) 3.95 (8H) 3.52 (4H) δ (S-C-CH_2) 3.43 (12H) δ (CH_2) 1.7, 2.7, 3.1 (t, 12H). ^{13}C NMR (300 MHz, δ D_2O) δ (–CH=N) 152.0, δ (S-C) 44.5, 40.2 δ (S-C-C) 24.1 δ (CH_2) 30.5, 40.5, 47.5.; IR (KBr, cm^{-1}) ν$(CH_2)_6$ 2899(s) ν(–CH=N) 1611(s); MS (*m/z*): $[RuCl]^+$ = 136, $[C_4H_8ClOSRu]^+$ = 240,$[C_{10}H_8N_2ClRu]^+$ = 292, $[C_{14}H_{16}N_2OSClRu]^+$ = 396, $[C_{34}H_{40}N_4OSClRu]^+$ = 689, $[C_{48}H_{56}N_6O_2S_2Cl_3Ru_2^{101}]^+$ = 1121, $[C_{48}H_{56}N_6O_2S_2Cl_3Ru_2^{102}]^+$ = 1123; Anal. calcd. (%) for $C_{52}H_{64}N_6O_3S_3Ru_2Cl_4$: C, 49.05; H, 5.24; N, 6.25; S, 7.44; Ru, 16.30; Found:C 49.51 H 5.10 N 6.63 S 7.62 Ru 16.05.

Antibacterial activity: All the precursor complexes and synthesized complexes were screened for antibacterial activity against Gram-negative bacteria *Escherichia coli* MTCC, 1304 at different concentrations using, Well Diffusion method by agar well diffusion method as described by Mehrotra *et al.* [15]. In brief, overnight grown bacterial cells (about 10^5 colony forming unit) were spread on Mueller Hinton (MH) agar plates by using sterile cotton swab. Uniform wells were created in agar slab by using cork borer. A 50 μL solution of test and control was placed in respective wells. It was interestingly observed that 0.01 % it showed less activity against *Escherichia coli* but at 0.02 and 0.03 % active inhibition zone was observed in comparison to chloramphenicol and they are active against the same bacteria (Table-1).

RESULTS AND DISCUSSION

The structure of the ligand given in Fig. 2 was illustrated on the basis of various studies. FAB-Mass spectra of ligand

TABLE-1
ANTIBACTERIAL SCREENING AGAINST *E. coli* RESULTS SHOWING COMPARATIVE ACTIVITY OF RUTHENIUM POLYPYRIDAL COMPLEXES AND LIGAND WITH CHLORAMPHENICOL

S. No.	Complex/Precursor	Activity against *E. coli*	*Diameter of inhibition zone (mm) ± SEM
2A	μ-BDH (Ligand)	+	08 ± 0.75
A_1.	[{*cis*,*fac*-$RuCl_2$(DMSO)phen}$_2$(μBDH)].DMSO	+	19 ± 0.5
1a.	[*cis*,*fac*-$RuCl_2$(DMSO)$_2$phen]	+	09 ± 0.8
A_2.	[{*trans*-$RuCl_2$(DMSO)phen}$_2$(μ-BDH)].DMSO	+	15 ± 1.0
2a.	[*trans*-$RuCl_2$(DMSO)$_2$phen]	+	08 ± 0.9
A_3.	[{*cis*,*fac*-$RuCl_2$(DMSO)bpy}$_2$(μ-BDH)].DMSO	+	17 ± 0.5
3a	[*cis*,*fac*-$RuCl_2$(DMSO)$_2$bpy]	+	08 ± 0.8
A_4.	[{*trans*-$RuCl_2$(DMSO)bpy}$_2$(μ-BDH)].DMSO	+	19 ± 1.0
4a.	[*trans*-$RuCl_2$(DMSO)$_2$bpy]	+	09 ± 0.9
A_5.	[{*cis*,*fac*-$RuCl_2$(TMSO)phen}$_2$(μ-BDH)]·TMSO	+	16 ± 1.0
5a.	[*cis*,*fac*-$RuCl_2$(TMSO) $_2$phen]	–	07 ± 0.5
A_6.	[{*trans*-$RuCl_2$(TMSO)phen}$_2$(μ-BDH)]·TMSO	+	21 ± 0.5
6a	[*trans*-$RuCl_2$(TMSO) $_2$phen]	+	08 ± 0.8
A_7.	[{*cis*,*fac*-$RuCl_2$(TMSO)bpy}$_2$(μ-BDH)]·TMSO	+	19 ± 0.5
7a	[*cis*,*fac*-$RuCl_2$(TMSO)$_2$bpy]	–	06 ± 0.5
A_8.	[{*trans*-$RuCl_2$(TMSO)bpy}$_2$(μ-BDH)]·TMSO	+	21 ± 1.0
8a	[*trans*-$RuCl_2$(TMSO) $_2$bpy]	+	09 ± 0.8
9.	Chloramphenicol	+	40 ± 0.94

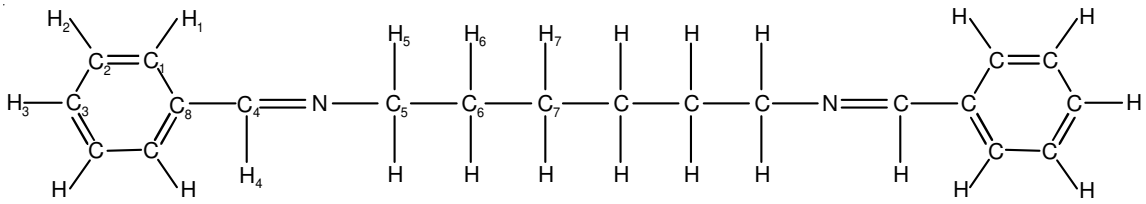

Fig. 2. Structure of ligand

shows pseudomolecular ion peak at *m/z* = 286 confirming the mole-cular weight of the ligand. In FT-IR spectra of the ligand a broad absorption band was observed at 2939 cm^{-1} assigned for methylene chain. The presence of azomethine group (>CH=N) was confirmed by a sharp peak at 1647 cm^{-1} [16,17].

In the ^1H NMR spectrum a signal for (>CH=N) group was observed at δ 8.80 ppm. Multiplets observed in the range δ 7.30-8.10 ppm were assigned for aromatic proton (Ar–H). The presence of methylene protons attributed by the presence of a triplet at δ 2.10, δ 3.20 and δ 3.60 ppm [18]. In ^{13}C NMR a signal at δ 161.0 ppm, was assigned for azomethine (>CH=N) group. The signals in the range δ 129-130 ppm were attributed for aromatic carbon. Singlets at δ 30, δ 51 and δ 60 ppm were assigned for methylene carbon [18,19].

In ^2D NMR spectra of ligand (Fig. 3) the aromatic carbon C-1 at δ 130.50 ppm is found connected to H-1 at δ 8.10 ppm, C-2 at δ 129.0 ppm is found connected to H-2 at δ 7.70 ppm. The carbon atom C-3 at δ 130.0 ppm is found connected to H-3 at δ 7.30 ppm C-8 is found to appear at δ 129 ppm. The azomethine carbon (>CH=N) C-4 appeared at δ 161 ppm is found connected to H-4 at δ 8.80 ppm. The six equivalent methylene carbons of hexane, C-5 at δ 61.0 ppm was found connected to H-5 at δ 3.6 ppm, C-6 at δ 51.0 ppm was found connected to H-6 at δ 3.20 ppm and the carbon C-7 at δ 30.0 ppm was connected to H-7 at δ 2.10 ppm.

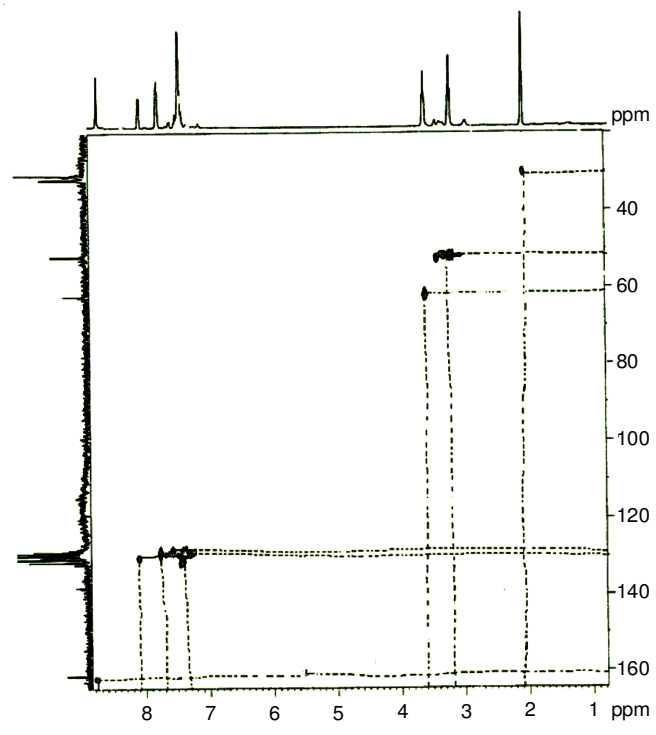

Fig. 3

Characterization of ruthenium complexes: Molecular weight and empirical formula of all the complexes were determined by FAB-Mass and elemental analyses. The low molecular conductance value between 41-56 Ω^{-1} cm^2 mol^{-1} for all the complexes in a dilute solution (about 0.001 M) were attributed to be non-electrolytic nature in the range suggested for 1:1 electrolyte [20,21]. The results are slightly higher than expected for non electrolyte, which is probably that in solution state one chloro ligand is replaced by solvent molecule, which leads to the formation of 1:1 electrolyte. Probably, second chloro ligand does not undergo exchange by another solvent molecule, thus it would not lead to formation of 2:1 electrolyte.

Electronic spectral study: All the complexes were diamagnetic (low spin d^6, S = 0) as expected for low spin ruthenium(II) complexes and displayed seven to ten bands in electronic spectra. Two/three less intense absorption bands observed in visible region between 623-664 nm and 490-579 nm were due to *d-d* transition corresponding to $^1A_1g \rightarrow {}^1T_1g$ and $^1A_1g \rightarrow {}^1T_2g$, respectively. Three to five bands with high extinction coefficient appeared between 410-478 nm were assigned to MLCT transition. Two MLCT transitions appear due to the existence of two different acceptor levels in 2,2'-bipyridyl/1,10-phenanthroline. Two bands in the range 375-408 nm were designated to intraligand transitions as π-π* and n-π* non-bonding electrons present on the nitrogen of the azomethine group in the Schiff base complexes respectively [21-24]. The enhancement (nearly more than double) of the absorbance in dinuclear complexes as compared to mononuclear precursor complexes could be considered in favour of presence of two ruthenium(II) centers.

Infrared spectral study: In all the complexes a downwards shift was observed by 25-30 cm^{-1} and also the peak intensity was decreased than the free ligand spectra indicating that the two metal center were symmetrically coordinated to the nitrogen of ligand. In the ligand a peak at 2939 cm^{-1} was observed for methylene chain which was also observed in all the complexes in the range 2905-2895 cm^{-1}. In all the complexes a peak observed in the range 1129-1085 cm^{-1} was assigned for ν(SO) [25-28]. Another peak observed in the range 1060-1040 cm^{-1} was assigned for uncoordinated DMSO/TMSO [17,18]. A weak band at about 450 cm^{-1} was assigned for ν(Ru–S).

^1H NMR spectra: A broad signal observed at about δ 9.80 ppm for 2 protons was attributed to the azomethine group (>CH=N). This signal was actually observed at higher δ value than that of ligand, which confirms the involvement of azomethine-N in coordination to the ruthenium metal center. In ^1H NMR of all Ru(II) complexes signals in the range δ 7.80-9.80 ppm were assigned for pyridyl protons and in range δ 3.64-3.35 ppm, δ 2.62-2.48 ppm and δ 2.12-2.00 ppm as a triplet, were assigned for 4 methylene protons each associated

with 5, 6, 7 carbon. In [*cis/trans* -$RuCl_2(SO)_2(N\text{-}N)$](L) one signal at about δ 3.40 ppm for 12 protons was attributed to methyl group of DMSO *anti* to Cl at both the ruthenium centers and at about δ 2.90 ppm for 12 protons was attributed to methyl group of DMSO *trans* to pyridyl-N of polypyridyl group. Three signals were observed in the TMSO analogues at about δ 4.20 ppm for 8 protons was attributed to S-CH_2 of TMSO situated anti to Cl at both ruthenium centers. The multiplet centered at about δ 3.60 ppm for 4 protons was assigned to S-CH_2 of free TMSO molecule. However, multiplet centered at about δ 3.40 ppm was assigned for all the 12 protons of S-C-CH_2 of TMSO [29-32].

^{13}C NMR spectra: In ^{13}C NMR, the ligand signal for azomethine carbon appeared at about δ 161 ppm which was shifted towards lower δ value in the complex and appeared at about δ 152 ppm confirming its involvement in co-ordination to the metal center also signals observed in the range δ 133.5-142 ppm were assigned for pyridyl carbon [17,18]. Similarly signals in the range of δ 120.0-131.5 ppm were attributed for the aromatic carbon [33,34].

{^{13}C-^{1}H}^{2}D NMR (HETCOR) spectrum: In {^{13}C-^{1}H}^{2}D NMR spectrum of [{*trans*-$RuCl_2$(DMSO)phen}$_2$(μ-BDH)]·DMSO in Fig. 4(a) and 4(b) signal in the range δ 134.0-139.0 ppm were assigned for pyridyl carbon which were connected to the pyridyl protons in the range δ 8.0-9.2 ppm as multiplet. The aromatic carbons were found in the range of δ 124-129 ppm, which were connected to the aromatic proton in the range δ 7.5-7.7 ppm. The methylene carbon of *n*-hexane appeared in the range δ 42-50 ppm, which were connected to the methylene proton at δ 2.06-3.50 ppm. The azomethine carbon

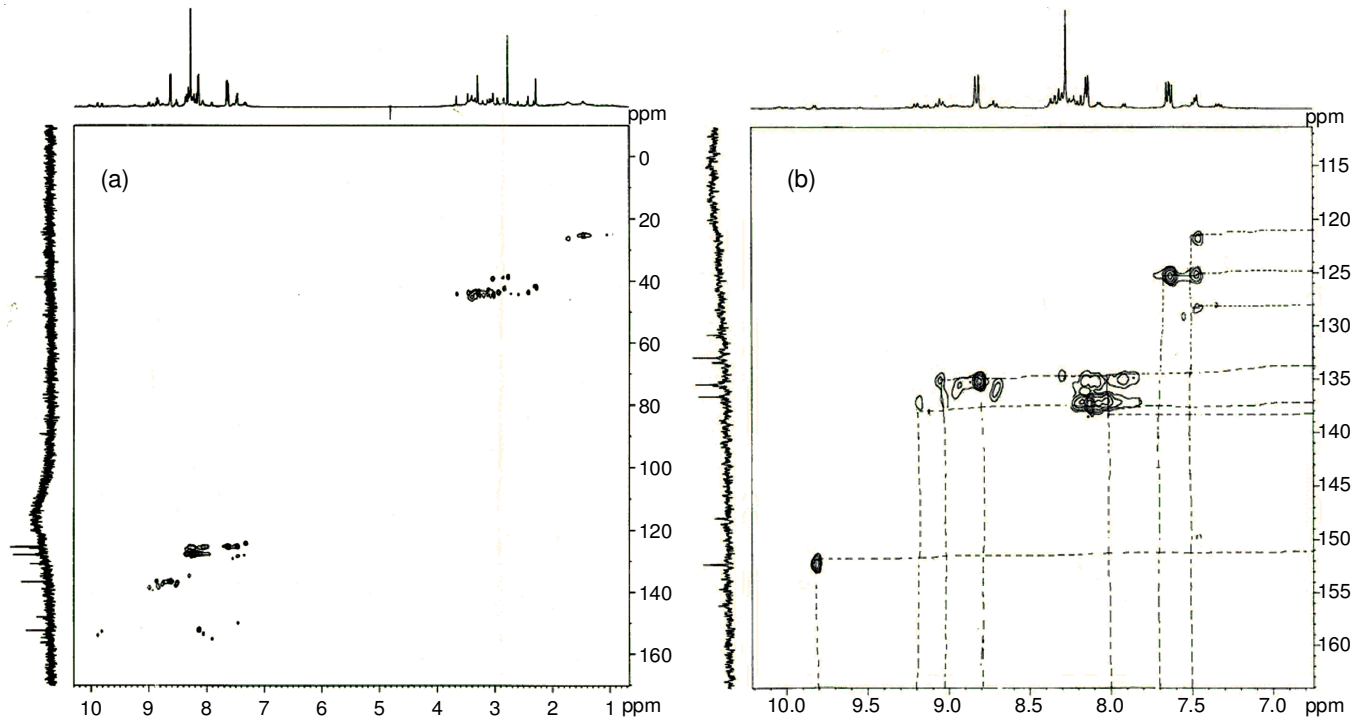

Fig. 4.

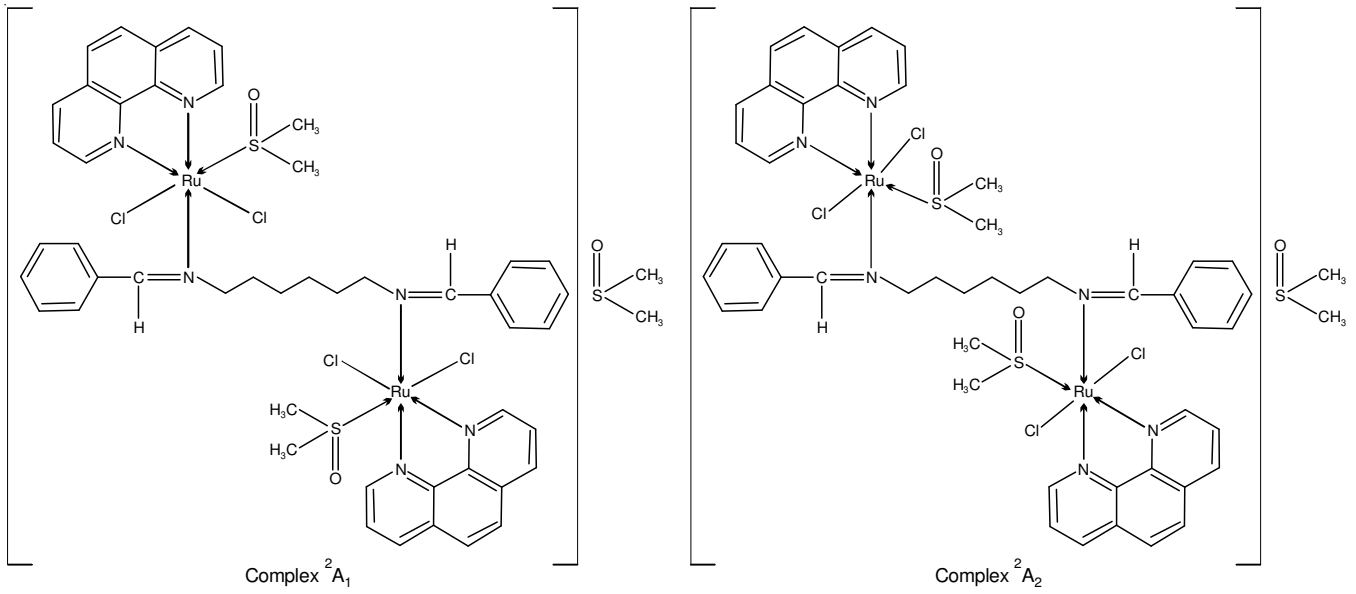

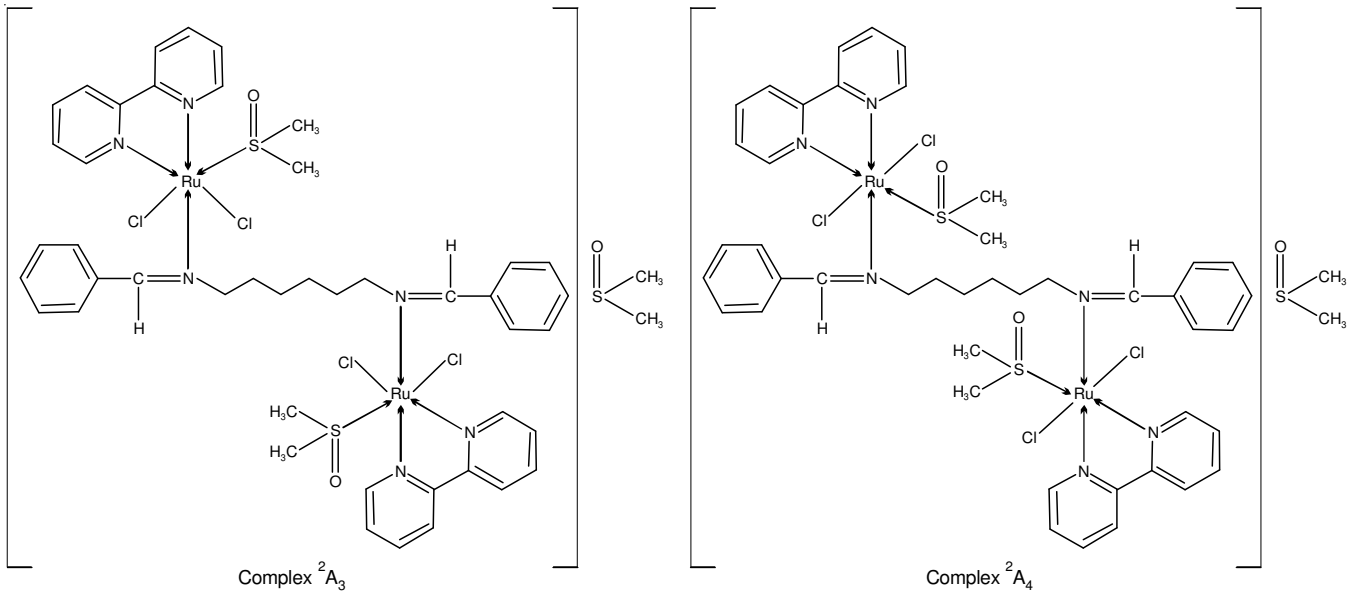

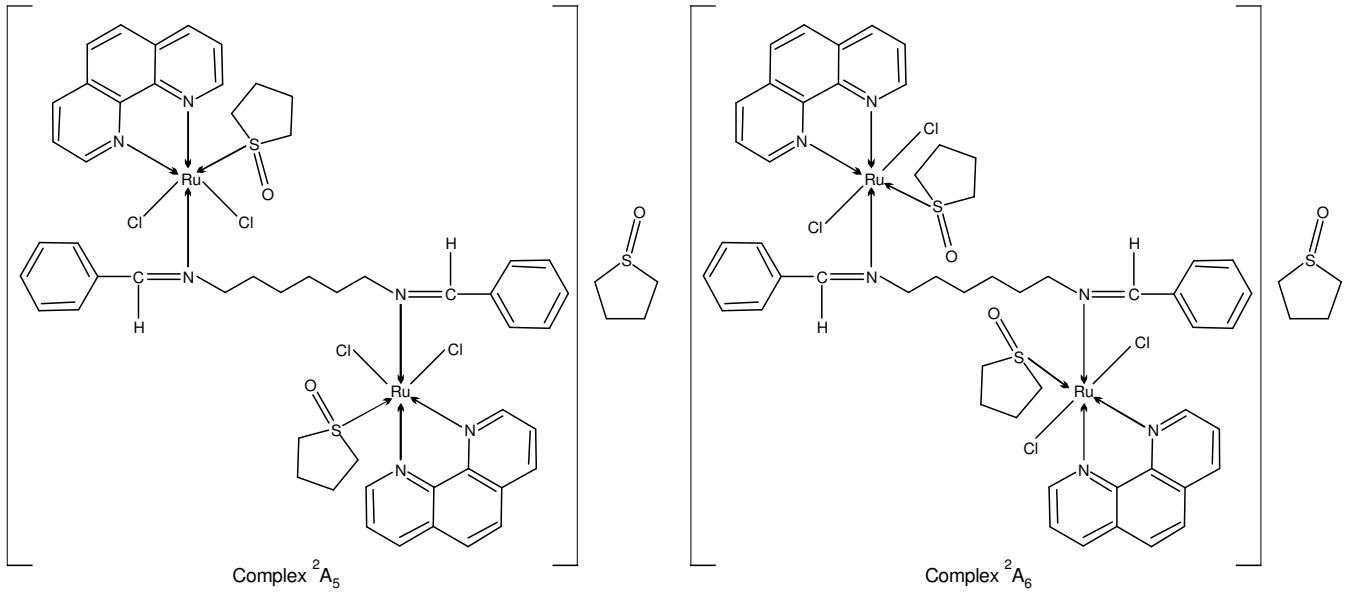

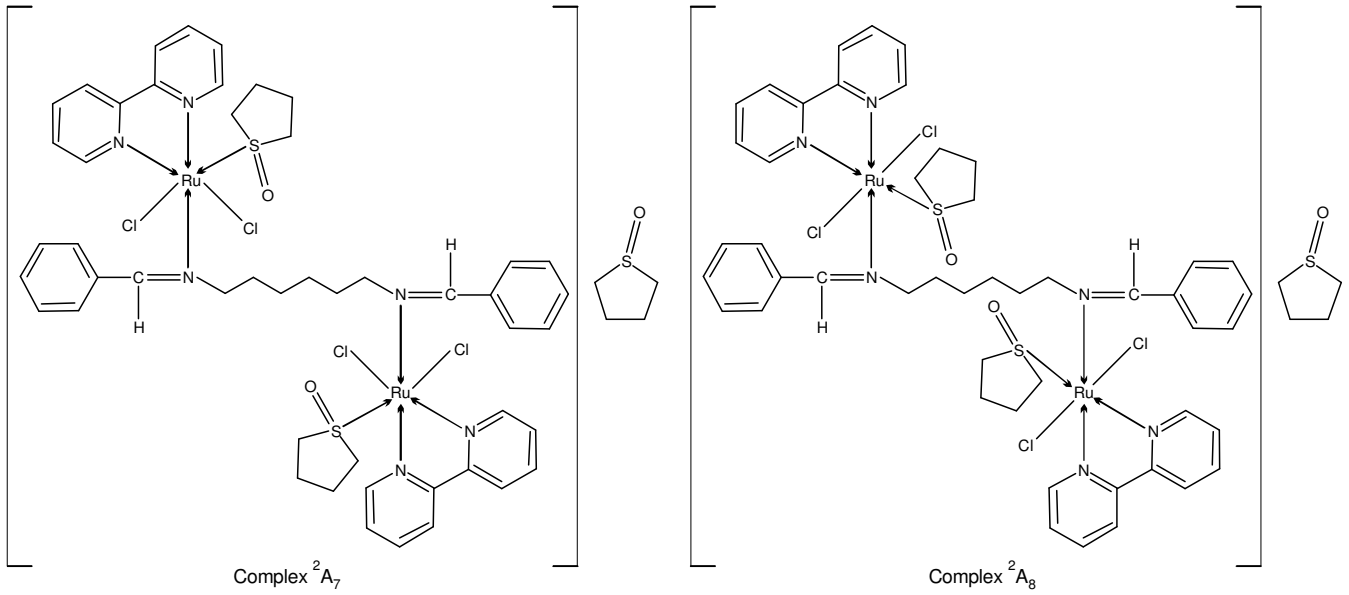

Fig. 5. Proposed structure of complexes $^2A_1$, $^2A_2$, $^2A_3$, $^2A_4$, $^2A_5$, $^2A_6$, $^2A_7$ and $^2A_8$

(>C=NH) was found to appear at δ 152 ppm connected to the azomethine proton at δ 9.80 ppm [35]. The peak at δ 44 ppm for the DMSO carbon was found connected to the DMSO methyl proton at δ 2.9 ppm, also in the uncoordinated DMSO molecule a peak of carbon at δ 36 ppm was found connected to DMSO methyl proton at δ 2.3 ppm.

Conclusion

Based on the charactization studies of the complexes, the tantative structures are shown in Fig. 5. All complexes and ligand were screened against bacteria but the ligand was found less potent than the synthesized complexes. All the screened complexes, A_1-A_8, inhibit the growth of bacteria and are found more potent than their precursors. This was probably due to the enhanced lipophilic nature of the complexes, which lead to the breakdown of permeability barriers of the cell and thus retard the normal cell process in bacteria.

ACKNOWLEDGEMENTS

The authors are thankful to The Principal, Govt. Model Science College, Jabalpur and Head, Department of Chemistry, Govt. Model Science College, Jabalpur for providing laboratory facilities. The authors are also indebted to Dr. K.K. Verma and Dr. K.K. Mishra, Retired Professors, Department of Chemistry, RDVV, Jabalpur, India for their help rendered in IR and UV spectra. Thanks are also due to SAIF, CDRI Lucknow, India for $\{^{13}C\text{-}^{1}H\}^{2}D$ NMR (HETCOR) spectral analysis, FAB mass and elemental analysis. The authors are also thankful to MPCOST, Bhopal, (M.P.), India for providing financial Assistance.

REFERENCES

1. F. Schramm, R. Chandrasekar, T.A. Zevaco, M. Rudolph, H. Görls, W. Poppitz and M. Ruben, *Eur. J. Inorg. Chem.*, 53 (2009); https://doi.org/10.1002/ejic.200800628.
2. V. Balzani, A. Juris, M. Venturi, S. Campagna and S. Serroni, *Chem. Rev.*, **96**, 759 (1996); https://doi.org/10.1021/cr941154y.
3. (a) J.M. Berg, J.L. Tymoczko and L. Stryer, Biochemistry, W.H. Freeman, New York, vol. 6 (2006).
(b) A.F. Collings and C, Critchley, Artificial Photosynthesis: From Basic Biology to Industrial Application, Wiley-VCH: Weinheim, Germany, (2005).
(c) M. Chen, K.P. Ghiggino, S.H. Thang and G.J. Wilson, *Angew. Chem. Int. Ed.*, **44**, 4368 (2005); https://doi.org/10.1002/anie.200462796.
(d) M.K. Nazeeruddin and M. Griaitzel, in eds.: J.A. McCleverty and T.J. Meyer, Comprehensive Coordination Chemistry II, Elsevier Amsterdam, vol. 9 (2003).
(e) A. Hagfeldt and M. Gratzel, *Acc. Chem. Res.*, **33**, 269 (2000); https://doi.org/10.1021/ar980112j.
(f) C.A. Bignozzi, J.R. Schoonover, F.A. Scandola, in ed.: G.J. Meyer, Progress in Inorganic Chemistry, Wiley: New York, vol. 44 (1999).
(g) L. Hammarstrom, *Curr. Opin. Chem. Biol.*, **7**, 666 (2003); https://doi.org/10.1016/j.cbpa.2003.10.002.
4. (a) F. Liu, J.J. Concepcion, J.W. Jurss, T. Cardolaccia, J.L. Templeton and T.J. Meyer, *Inorg. Chem.*, **47**, 1727 (2008); https://doi.org/10.1021/ic701249s.
(b) T. Meyer, *Nature*, **451**, 778 (2008); https://doi.org/10.1038/451778a.
(c) S. Rau, B. Schafer, D. Gleich, E. Anders, M. Rudolph, M. Friedrich, H. Gorls, W. Henry and J.G. Vos, *Angew. Chem. Int. Ed.*, **45**, 6215 (2006); https://doi.org/10.1002/anie.200600543.
5. (a) M.K. Nazeeruddin, S.M. Zakeeruddin, J.J. Lagref, P. Liska, P. Comte, C. Barolo, G. Viscardi, K. Schenk and M. Graetzel, *Coord. Chem. Rev.*, **248**, 1317 (2004); https://doi.org/10.1016/j.ccr.2004.03.012.
(b) M.K. Nazeeruddin, C. Klein, P. Liska and M. Grätzel, *Coord. Chem. Rev.*, **249**, 1460 (2005); https://doi.org/10.1016/j.ccr.2005.03.025.
(c) F.T. Kong, S.Y. Dai and K.J. Wang, *Chin. J. Chem.*, **25**, 168 (2007); https://doi.org/10.1002/cjoc.200790034.
6. (a) J.D. Badjic, C.M. Ronconi, J.F. Stoddart, V. Balzani, S. Silvi and A. Credi, *J. Am. Chem. Soc.*, **128**, 1489 (2006); https://doi.org/10.1021/ja0543954.
(b) A. Petitjean, F. Puntoriero, S. Campagna, A. Juris and J.M. Lehn, *Eur. J. Inorg. Chem.*, 3878 (2006); https://doi.org/10.1002/ejic.200600466.
(c) V. Balzani, G. Bergamini, F. Marchioni and P. Ceroni, *Coord. Chem. Rev.*, **250**, 1254 (2006); https://doi.org/10.1016/j.ccr.2005.11.013.
(d) S. Nitahara, N. Terasaki, T. Akiyama and S. Yamada, *Thin Solid Films*, **499**, 354 (2006); https://doi.org/10.1016/j.tsf.2005.07.014.
7. (a) V. Balzani, A. Credi, S. Silvi and M. Venturi, *Chem. Soc. Rev.*, **35**, 1135 (2006); https://doi.org/10.1039/b517102b.
(b) V. Balzani, M. Clemente-Leon, A. Credi, B. Ferrer, M. Venturi, A.H. Flood and J.F. Stoddart, *Proc. Natl. Acad. Sci. USA*, **103**, 1178 (2006); https://doi.org/10.1073/pnas.0509011103.
(c) V. Balzani, M. Venturi and A. Credi, In Molecular Devices and Machines-A Journey in the Nano World, Wiley-VCH: Weinheim, Germany (2003).
8. E. Corral, A.C.G. Hotze, D.M. Tooke, A.L. Spek and J. Reedijk, *Inorg. Chim. Acta*, **359**, 830 (2006); https://doi.org/10.1016/j.ica.2005.05.017.
9. Z. Ganbaatar, S.A. Osadchii, É.É. Shul'ts, T.G. Tolstikova, M.P. Dolgikh and G.A. Tolstikov, *Pharm. Chem. J.*, **36**, 478 (2002); https://doi.org/10.1023/A:1021892621783.
10. D. Mlynarcik, F. Devinsky and I. Lacko, *Folia Microbiol.*, **24**, 188 (1979); https://doi.org/10.1007/BF02927306.
11. I.P. Evans, A. Spencer and G. Wilkinson, *J. Chem. Soc., Dalton Trans.*, 204 (1973); https://doi.org/10.1039/DT9730000204.
12. E. Alessio, G. Mestroni, G. Nardin, W.M. Attia, M. Calligaris, G. Sava and S. Zorzet, *Inorg. Chem.*, **27**, 4099 (1988); https://doi.org/10.1021/ic00296a006.
13. E. Alessio, B. Milani, G. Mestroni, M. Calligaris, P. Faleschini and W.M. Attia, *Inorg. Chim. Acta*, **177**, 255 (1990); https://doi.org/10.1016/S0020-1693(00)85984-8.
14. E. Alessio, G. Balducci, M. Calligaris, G. Costa, W.M. Attia and G. Mestroni, *Inorg. Chem.*, **30**, 609 (1991); https://doi.org/10.1021/ic00004a005.
15. R. Mehrotra, S.N. Shukla, P. Gaur and A. Dubey, *Eur. J. Med. Chem.*, **50**, 149 (2012); https://doi.org/10.1016/j.ejmech.2012.01.049.
16. R.M. Silverstein, G.C. Bassler and T.C. Morrill, Spectrometric Identification of Organic Compouds, John Wiley & Sons, Inc, New York, pp. 123-131, 219-262 (1991).
17. P.S. Kalsi, Spectroscopy of Organic Compounds, New Age International Ltd., pp. 206-210, 246-256, 342-350 (2005).
18. J.M. Miller and K. Balasanmugam, *Can. J. Chem.*, **67**, 1496 (1989); https://doi.org/10.1139/v89-228.
19. N.G. Tsierkezos, U. Ritter, A.I. Philippopoulos and D. Schroder, *J. Coord. Chem.*, **63**, 3517 (2010); https://doi.org/10.1080/00958972.2010.516362.
20. K.D. Keerthi, B.K. Santra and G.K. Lahiri, *Polyhedron*, **17**, 1387 (1998); https://doi.org/10.1016/S0277-5387(97)00277-5.
21. S.N. Shukla, P. Gaur, R. Mehrotra, M. Prasad, H. Kaur, M. Prasad and R.S. Srivastava, *J. Coord. Chem.*, **62**, 2556 (2009); https://doi.org/10.1080/00958970902862628.
22. U.C. Sarma and R.K. Poddar, *Polyhedron*, **7**, 1737 (1988); https://doi.org/10.1016/S0277-5387(00)80405-2.
24. A.B.P. Lever, Inorganic Electronic Spectroscopy, Elsevier, Amsterdam, The Netherlands (1984).
25. S. Dutta and P.K. Bhattacharya, *Indian J. Chem.*, **42A**, 262 (2003).
26. R.S. Srivastava, F.R. Fronczek and L.M. Romero, *Inorg. Chim. Acta*, **357**, 2410 (2004); https://doi.org/10.1016/j.ica.2004.01.026.

27. T. Bora and M.M. Singh, *J. Inorg. Nucl. Chem.,* **38**, 1815 (1976); https://doi.org/10.1016/0022-1902(76)80095-4.
28. W.L. Reynolds, in ed.: S.J. Lippard, Dimethyl Sulfoxide in Inorganic Chemistry, In: Progress in Inorganic Chemistry, John Wiley & Sons, Inc., Hoboken, NJ, USA, vol. 12 (1970): https://doi.org/10.1002/9780470166130.ch1.
29. J.A. Davis, in eds.: H.J. Emeléus and A.G. Sharpe, Advances in Inorganic Chemistry and Radiochemistry, Elsevier, vol. 24, p. 115 (1981).
30. E. Alessio, *Chem. Rev.*, **104**, 4203 (2004); https://doi.org/10.1021/cr0307291.
31. P.K.L. Chan, B.R. James, D.C. Frost, P.K.H. Chan, H.L. Hu and K.A. Skov, *Can. J. Chem.*, **67**, 508 (1989); https://doi.org/10.1139/v89-078b.
32. F.D. Rochon, P.C. Kong and L. Girard, *Can. J. Chem.*, **64**, 1897 (1986); https://doi.org/10.1139/v86-313.
33. P. Kumar, A. K. Singh, M. Yadav, P. Li, S. K. Singh, Q. Xu, D.S. Pandey, *Inorg. Chim. Acta*, **368**, 124 (2011); https://doi.org/10.1016/j.ica.2010.12.057.
34. J.D. Oliver and D.P. Riley, *Inorg. Chem.*, **23**, 156 (1984); https://doi.org/10.1021/ic00170a009.
35. N.P.E. Barry, O. Zava, J. Furrer, P.J. Dyson and B. Therrien, *Dalton Trans.*, **39**, 5272 (2010); https://doi.org/10.1039/c001521k.
36. H.J. Guadalupe, J. Narayanan and T. Pandiyan, *J. Mol. Struct.*, **989**, 70 (2011); https://doi.org/10.1016/j.molstruc.2011.01.005.